

Environments of galaxies in groups within the supercluster-void network

H. Lietzen¹, E. Tempel^{2,3}, P. Heinämäki¹, P. Nurmi¹, M. Einasto³, and E. Saar³

¹ Tuorla Observatory, Department of Physics and Astronomy, University of Turku, Väisäläntie 20, 21500 Piikkiö, Finland

² National Institute of Chemical Physics and Biophysics, Tallinn 10143, Estonia

³ Tartu Observatory, 61602 Tõravere, Tartumaa, Estonia

Received / Accepted

ABSTRACT

Context. Majority of all galaxies reside in groups of less than 50 member galaxies. These groups are distributed in various large-scale environments from voids to superclusters.

Aims. Evolution of galaxies is affected by the environment in which they reside. Our aim is to study the effects that the local group scale and the supercluster scale environment have on galaxies.

Methods. We use a luminosity-density field to determine density of the large-scale environment of galaxies in groups of various richness. We calculate fractions of different types of galaxies in groups with richnesses up to 50 member galaxies and in different large-scale environments from voids to superclusters.

Results. The fraction of passive elliptical galaxies rises and the fraction of star-forming spiral galaxies declines when the richness of a group of galaxies rises from two to approximately ten galaxies. On the large scale, the passive elliptical galaxies become more numerous than star-forming spirals when the environmental density grows to the density level typical for superclusters. The large-scale environment affects the level of these fractions in groups: galaxies in equally rich groups are more likely to be elliptical in supercluster environments than in lower densities. The crossing point, where the number of passive and star-forming galaxies is equal, happens in groups with lower richness in superclusters than in voids. Galaxies in low-density areas require richer groups to evolve from star-forming to passive. Groups in superclusters are on average more luminous than groups in large-scale environments with lower density. These results imply that the large-scale environment affects the properties of galaxies and groups.

Conclusions. Our results suggest that the evolution of galaxies is affected by both, by the group in which the galaxy resides, and by its large-scale environment. Galaxies in lower-density regions develop later than galaxies in similar mass groups in high-density environments.

Key words. large-scale structure of Universe – galaxies: groups: general – galaxies: statistics

1. Introduction

Galaxies form groups and clusters of various sizes. These groups and clusters are distributed in different environments on the large scale. Regions of high galaxy density are superclusters, which are surrounded by filaments and low-density void areas.

The properties of galaxies are affected by their cluster or group-scale environment. In group environments, galaxies experience baryonic processes, such as ram pressure stripping (Gunn & Gott 1972), viscous stripping and strangulation (Larson et al. 1980), and gravitational effects, such as galaxy tidal interactions with other galaxies and the cluster potential (Moore et al. 1996), and galaxy merging. These local processes are believed to modify galaxy morphologies from spiral galaxies to gas poor and spheroidal ones (Gunn & Gott 1972; Dressler 1980; Postman & Geller 1984). According to the morphology-density relation, elliptical galaxies are more concentrated in centers of clusters than spiral galaxies (Dressler 1980; Postman & Geller 1984). Similarly galaxies in higher densities are more luminous (Hamilton 1988), and have lower star-formation rates (Gómez et al. 2003). The dependency of the star-formation rate or color with the environment is stronger than the dependency between morphology and the environment (Kauffmann et al. 2004; Blanton et al. 2005). According to Baldry et al. (2006), the environmental dependence is at least as important as stellar mass in determining the fraction of

red galaxies in a population. Finally, different types of active galactic nuclei (AGN) appear in different local environments (Hickox et al. 2009).

Besides the local group or cluster scale, the properties of galaxies depend also on their environment on the large scale. The large-scale morphology density relation was first found by Einasto & Einasto (1987). According to Balogh et al. (2004), the fraction of red galaxies is higher where the surface density of galaxies is higher. Porter et al. (2008) have found that star-formation rate of galaxies depend on their location in large-scale filaments. Skibba et al. (2009) found significant color-environment correlations on $10 h^{-1} \text{Mpc}$ scale in both, spiral and elliptical galaxies. Tempel et al. (2011) derived luminosity functions of spiral and elliptical galaxies in different large-scale environments. They found that the luminosity function of elliptical galaxies depends strongly on environment, while for spiral galaxies the luminosity function is almost independent of the large-scale environment. The large-scale environments of AGN were studied by Lietzen et al. (2011). In the same way as in smaller scale, radio galaxies favor high-density environments, while radio-quiet quasars and Seyfert galaxies are mostly in low-density regions.

In high-density large-scale environments the groups and clusters of galaxies tend to be larger and more massive than in low-density environments (Einasto et al. 2005b). Because of

this, group-scale effects are also present when studying the large-scale environments. The effects on galaxy properties on different scales up to tens of Mpc can be distinguished using a luminosity-density method (Einasto et al. 2003). Group and supercluster scale environments of galaxies have earlier been studied together by Einasto et al. (2008). They found that in outskirts regions of superclusters, rich groups contain more late-type galaxies than in the supercluster cores, where the rich groups are populated mostly by early-type galaxies. Einasto et al. (2007) found that in the high-density cores of rich superclusters there is an excess of early type galaxies in groups and clusters as well as among galaxies that do not belong to any group. According to Einasto et al. (2012a), isolated clusters are poorer than supercluster members.

Some studies have used the number-density of galaxies to study the large-scale environments of galaxies. In these studies the large scale usually refers to scales of a few Mpc. Zandivarez & Martínez (2011) found that the Schechter parameters of galaxies in groups at high-density environments do not depend on the mass of the group, while in low-density regions some variation occurs. On the other hand, Blanton & Berlind (2007) found that on a few Mpc scales the environment is only weakly related to colors of galaxies, while the small-scale environment matters more. Wilman et al. (2010) found no correlation at scales of ~ 1 Mpc and even an anticorrelation on scales of 2–3 Mpc in the fraction of red galaxies.

Of the different ways of determining the environment of a galaxy, some are sensitive to the local scales, which depend on the size of the dark matter halo surrounding the galaxy. Other methods are more sensitive to large scales, which represents the environment in the supercluster-void network (Haas et al. 2011; Muldrew et al. 2012). In this paper, we use spectroscopic galaxy and group catalogs based on the Sloan Digital Sky Survey (SDSS) to study the environments of galaxies in groups on local and large scale. As a measure for the local scale environment we use the richness of the group, and for the large scale environment a luminosity density field smoothed to scales typical to superclusters. Our goal is to distinguish between the effects that different scales of environment have on galaxies.

The paper is composed as follows: In Sect. 2 we present the data, and describe how the group catalog and the large-scale luminosity-density field were constructed. We also describe the galaxy classification criteria. In Sect. 3 we present our results on the environments of galaxies on group scale and on the large scale. In Sect. 4 we compare our results to previous studies and discuss the possible implications of our results on galaxy evolution.

Throughout this paper we assume a cosmological model with the total matter density $\Omega_m = 0.27$, dark energy density $\Omega_\Lambda = 0.73$, and the Hubble constant $H_0 = 100 h \text{ km s}^{-1} \text{ Mpc}^{-1}$ (Komatsu et al. 2011).

2. Data

2.1. Galaxy and group sample

We used flux-limited galaxy and group catalogs based on the eighth data release (DR8) of the SDSS (York et al. 2000; Aihara et al. 2011). The details of the galaxy and group catalogs used in this study are given in Tempel et al. (2012). We determine groups of galaxies using the friend-of-friend cluster analysis that was introduced in cosmology by Turner & Gott (1976). This method was named friends-of-friends (FoF) by Press & Davis (1982). With the FoF method, galaxies are linked

into groups using a certain linking length. In a flux-limited sample the density of galaxies slowly decreases with distance. To take this selection effect properly into account we rescaled the linking length with distance, calibrating the scaling relation by observed groups (see Tago et al. 2008, 2010, for details). The linking length in our group finding algorithm increases moderately with distance.

The most important problem in obtaining the catalogues of systems of galaxies has been the inhomogeneity of the resulting samples due to selection effects in search procedures. The choice of the method and parameters depends on the goal of the study. For example, Berlind et al. (2006) applied the FoF method to the volume-limited samples of the SDSS with the goal to measure the group multiplicity function and to constrain dark matter halos. Yang et al. (2007) applied a halo-based group finder to study the relation between galaxies and dark matter halos over a wide dynamic range in halo masses. Our goal is to use groups and clusters for large-scale structure studies. In this respect, our group catalog are rather homogeneous: the group richnesses, mean sizes and velocity dispersions practically do not depend on their distance.

Since the data are magnitude limited, it causes distance-dependent selection effects: in farther distances, only the most luminous galaxies are detected. The luminosity-dependency causes also a color and/or morphology dependency, as the red and elliptical galaxies tend to be more luminous than blue and spiral galaxies. To reduce the distance effects we limited our data between distances 120 and $340 h^{-1} \text{ Mpc}$ (in redshift range 0.04–0.116). This is the most reliable part of the galaxy data. At distances less than $120 h^{-1} \text{ Mpc}$, there are extremely rich clusters that are not seen at larger distances. At distances of more than $340 h^{-1} \text{ Mpc}$ the richness of groups drops down rapidly (Tago et al. 2010). After limiting the distance, our data contains 306 397 galaxies which belong to 45 922 groups. Despite this limitation, the average color of galaxies still depends on the distance. The average $g-r$ color of galaxies with distance from 120 to $140 h^{-1} \text{ Mpc}$ is 2.3, while for galaxies from 320 to $340 h^{-1} \text{ Mpc}$ it is 2.9.

The apparent magnitude m (corrected for the Galactic extinction) was transformed into the absolute magnitude M according to the usual formula

$$M_\lambda = m_\lambda - 25 - 5 \log_{10}(d_L) - K, \quad (1)$$

where d_L is the luminosity distance in units of $h^{-1} \text{ Mpc}$, K is the $k+e$ -correction, and the index λ refers to the *ugriz* filters. The k -corrections were calculated with the KCORRECT (v4.2) algorithm (Blanton & Roweis 2007) and the evolution corrections were estimated, using the luminosity evolution model of Blanton et al. (2003). The magnitudes correspond to the rest-frame (at the redshift $z = 0$).

2.2. Estimating the environmental densities

As a measure of the large-scale environment we use a luminosity-density field that is smoothed to scales characteristic to superclusters. To construct the luminosity-density field, the luminosities of galaxies are corrected by a weighting factor in order to take into account the luminosities of galaxies outside the magnitude window of the survey. The weighting factor $W_L(d)$ is defined as

$$W_L(d) = \frac{\int_0^\infty L\phi(L) dL}{\int_{L_1(d)}^{L_2(d)} L\phi(L) dL}, \quad (2)$$

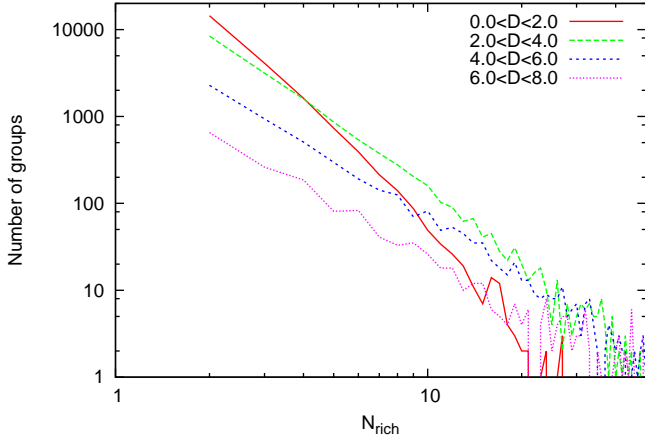


Fig. 1. The number of groups of different richnesses in four levels of large-scale density D .

where $L_{1,2} = L_{\odot} 10^{0.4(M_{\odot} - M_{1,2})}$ are the luminosity limits of the observational window at the distance d , corresponding to the absolute magnitude limits of the window M_1 and M_2 ; we took $M_{\odot} = 4.64$ mag in the r -band (Blanton & Roweis 2007). $\phi(L)$ denotes the galaxy luminosity function. The luminosity function was calculated as described in Tempel et al. (2011), and it can be approximated by the double power-law

$$\phi(L)d(L) \propto (L/L^*)^{\gamma} (L/L^*)^{(\delta-\alpha)/\gamma} d(L/L^*), \quad (3)$$

where α is the exponent at low luminosities, δ is the exponent at high luminosities, γ determines the speed of the transition between the two power laws, and L^* is the characteristic luminosity of the transition. The used parameters are: $\alpha = -1.305$, $\delta = -7.13$, $\gamma = 1.81$, and $M^* = -21.75$ (corresponds to L^*): this function is consistent with the luminosity function derived in Blanton et al. (2003).

After correcting for the luminosities, the luminosity-density field is then calculated on a cartesian grid using a $8 h^{-1} \text{Mpc}$ B3-spline smoothing kernel, which corresponds to the supercluster scale (Liivamägi et al. 2012). The density values (D) are normalized so that the densities are shown in units of the mean density of the field. Details on how the density field is calculated are given in Liivamägi et al. (2012). Regions with the large-scale density $D > 5.0$ can be defined as superclusters.

While calculating the density field, we also suppress the finger-of-god redshift distortions using the rms sizes of galaxy groups in the sky and their rms radial velocities. Tempel et al. (2012) showed that this procedure makes the galaxy distribution in groups approximately spherical, as intended.

We refer to Liivamägi et al. (2012) and Tempel et al. (2012) for more details how the density field is calculated.

Figure 1 shows the numbers of groups with different richnesses in different levels of D . Densities $0.0 < D < 2.0$ are characteristic for void regions, $2.0 < D < 4.0$ are typically filaments, $4.0 < D < 6.0$ are edges of superclusters, and the densities $6.0 < D < 8.0$ are supercluster core areas. The total number of galaxies in areas with $D > 8.0$ is low, since the densest cores are small in volume. Because of this, we do not analyze these regions here. Figure 1 shows that in void areas, groups are predominantly poorer than in denser large-scale environments.

2.3. Spectral and morphological classification

Active galaxies in the SDSS DR8 are divided in classes by their spectral emission lines using the criteria by Brinchmann et al. (2004). The classification is based on emission line ratios $[\text{O III}]/\text{H}\beta$ and $[\text{N II}]/\text{H}\alpha$. Galaxies with very weak or no emission lines are defined unclassifiable. We use this class as our sample of passive galaxies. Of the galaxies with strong emission lines, star-forming galaxies and AGN were distinguished by criteria found by Kewley et al. (2001) and Kauffmann et al. (2003). In this work, we use the AGN and star-forming galaxies, but not galaxies with composite spectra that have features between the two classes. We also omit galaxies with low S/N classification as star-forming or AGN. Our data consists of 84 427 passive galaxies, 89 713 star-forming galaxies, and 9 773 AGN.

We use the morphology classification that is carried out in Tempel et al. (2011). This classification takes into account the SDSS model fits, apparent ellipticities (and apparent sizes), and different galaxy colors. Additionally, the morphology is combined with the probabilities of being elliptical or spiral galaxies given by Huertas-Company et al. (2011). Tempel et al. (2012) showed that this classification agrees well with the Huertas-Company et al. (2011) classification. In our classification, the galaxies are divided into spirals, ellipticals/S0, and galaxies with uncertain classification. We drop galaxies with uncertain classification out of our sample, and get 37 683 passive ellipticals, 15 614 passive spirals, 1 513 star-forming ellipticals, and 78 566 star-forming spirals. For about 47% of the galaxies, the classification is unclear. The reason is twofold. Firstly, our classification in Tempel et al. (2011) is conservative and secondly, we use only galaxies, where Huertas-Company et al. (2011) classification agrees with our classification. Hence, our classification is rather conservative and leaves out uncertain galaxies that may influence our analysis.

According to Fukugita et al. (2004), approximately 3% of early-type galaxies are star-forming. On the other hand, Bamford et al. (2009) have found that of the red (non-star-forming) galaxies, 67% have early-type morphology. Our data has a similar distribution: passive elliptical galaxies make approximately 70% of passive galaxies, and approximately 4% of elliptical galaxies are star-forming.

Figure 2 shows the fractions of different types of galaxies at different redshifts. The fractions were calculated in bins of $z = 0.01$. The number of star-forming spiral galaxies declines strongly with increasing distance. Also, further away galaxies are smaller and appear rounder in the sky, which makes it harder to classify the galaxies. Because of this, the number of galaxies with unknown morphology increases with distance. This means that there are distance-dependent effects in our results. This is caused by the magnitude-limited data. Since the passive elliptical galaxies tend to be more luminous than the star-forming spiral, they can be observed from higher distances. The distance range of our data, 120 to $340 h^{-1} \text{Mpc}$ or 0.04 to 0.116 in redshift, corresponds to ~ 0.6 Gyr, and it is small enough to exclude significant evolutionary effects within the data.

3. Results

3.1. Large-scale environments

Basic environmental properties of our five data samples are shown in Table 1. The Table gives the number of galaxies in each sample, average colors of the galaxies, and the average group richness N_{rich} and large-scale density D in the environment of

Sample	N	$\langle g-r \rangle$	$\langle N_{\text{rich}} \rangle$	$\langle D \rangle$
Passive elliptical	37683	0.796 ± 0.001	10.0 ± 0.2	3.19 ± 0.02
Star-forming elliptical	1513	0.70 ± 0.008	4.2 ± 0.3	2.32 ± 0.05
Passive spiral	15614	0.776 ± 0.002	12.4 ± 0.3	3.3 ± 0.03
Star-forming spiral	78566	0.512 ± 0.001	4.5 ± 0.1	2.1 ± 0.01
AGN	9773	0.737 ± 0.002	6.6 ± 0.3	2.58 ± 0.03

Table 1. Statistics of the galaxy samples: Number of galaxies (N), average color ($\langle g-r \rangle$), average group richness ($\langle N_{\text{rich}} \rangle$), and average large-scale density ($\langle D \rangle$).

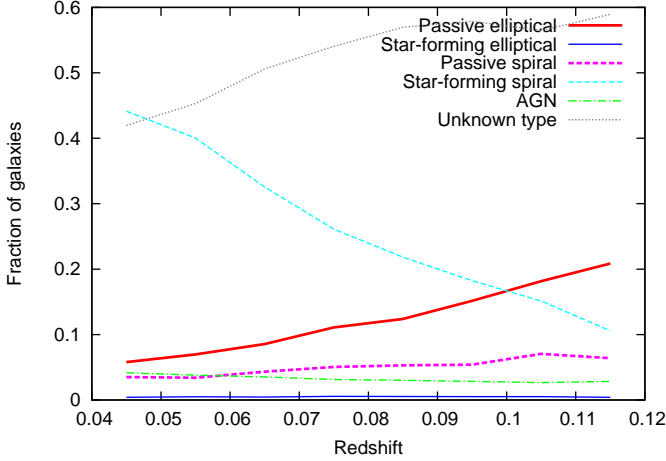


Fig. 2. Fractions of different types of galaxies as a function of redshift.

the different types of galaxies. The data shown here includes galaxies in all group richnesses from field galaxies to clusters of more than a hundred galaxies. Errors are standard errors of the average.

Table 1 shows that passive galaxies with both, elliptical and spiral morphology have higher density environments than star-forming galaxies. AGN settle in between: they have slightly richer environments than star-forming galaxies, but not as rich as the passive. Pasquali et al. (2009) also found that optically selected AGN reside in more massive halos than star-forming galaxies, but less massive than radio-emitting galaxies. The differences can be seen on both, the group scale and the large scale. From these values alone, we cannot see which scale is the main cause of the differences.

Figure 3 shows the average relative large-scale density for the galaxy samples as a function of group richness. Galaxies are divided in bins by the richness of groups where they reside with binning of ten galaxies. The average large-scale environmental density is calculated for galaxies in each class in each bin. The density is divided by the average density of galaxies of all types in the richness bin. As a result, we see how the environments of different types differ from the average environment of all galaxies. With the same group richness, passive galaxies always have higher density environments than star-forming galaxies and AGN. There is very little difference between the large-scale environments of spiral and elliptical passive galaxies. The similarity in environments of passive galaxies of both morphological types is supported by the group-scale results based on Galaxy Zoo (Bamford et al. 2009; Skibba et al. 2009), and STAGES (Wolf et al. 2009). For AGN in the smallest groups the large-scale density is higher than for spiral star-forming galaxies. In richer groups, AGN and star-forming galaxies have approximately equal large-scale densities.

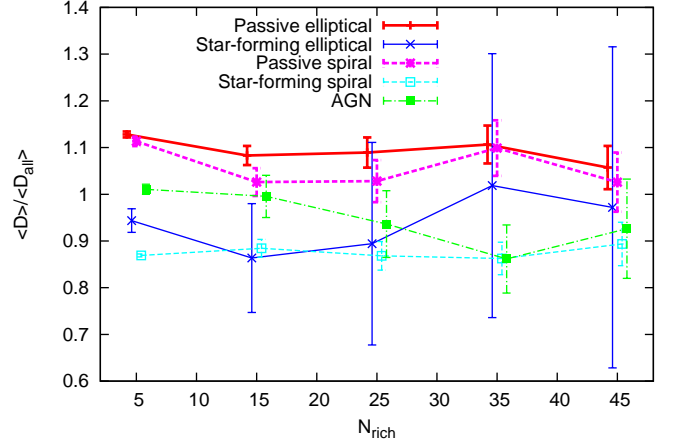


Fig. 3. Relative large-scale environments of different types of galaxies. The average large-scale density of each type divided by the average density of all galaxies is shown as a function of group richness. The error bars show Poisson errors.

The relative fractions of different types of galaxies in different large-scale density levels are shown in Fig. 4. The number of galaxies of each type was counted in each bin of 1.0 mean densities. The fraction of each type was then calculated by dividing this number by the number of all galaxies in the bin (including galaxies with unknown classification). All galaxies are more commonly in low-density regions, as was seen in Fig. 1. The error bars shown in Fig. 4 are Poisson errors, and since the number of galaxies is high, the errors are small. The top panel of the figure shows the distribution of all galaxies in the magnitude-limited sample between distances 120 and $340 h^{-1} \text{Mpc}$. To study the possible distance effects that may be caused by the magnitude-limited sample, we did the same calculation for a volume-limited sample (bottom panel of Fig. 4). The volume-limited sample was formed by a cut at absolute magnitude $M_r = -19$ and a distance cut at $225 h^{-1} \text{Mpc}$. There are no significant differences between the volume and magnitude-limited samples.

The fractions of different types of galaxies presented Fig. 4 show that when moving towards higher large-scale densities, the fraction of passive galaxies rise while the fraction of star-forming galaxies drops. Passive elliptical galaxies become more numerous than spiral star-forming galaxies at the density level of five times the mean density, which is approximately the lower limit for supercluster regions. Also the fraction of passive spiral galaxies rises towards higher densities.

The fraction of AGN is equally small at all densities. According to the Kolmogorov-Smirnov test, the relation between the large-scale density and the fraction of AGN does not differ significantly from a random sample of galaxies of the same size.

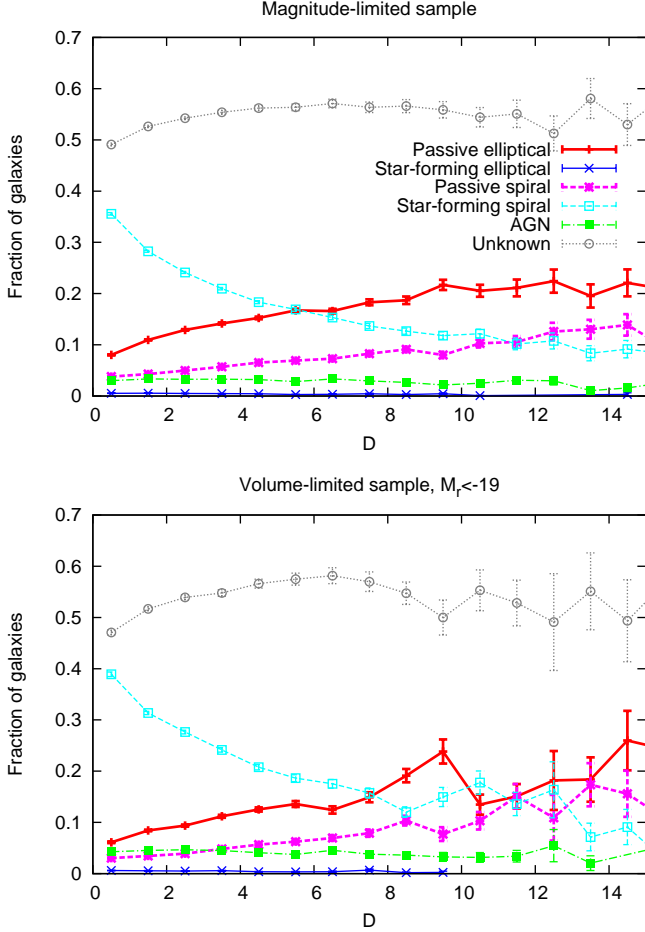


Fig. 4. Fractions of different samples of galaxies as a function of the large-scale environmental density. Top panel shows the fractions for the complete magnitude-limited sample of galaxies between distances 120 and $340 h^{-1}\text{Mpc}$. Bottom panel shows the fractions in a volume-limited sample with $M_r < -19$ and distance between 120 and $225 h^{-1}\text{Mpc}$. The numbers of galaxies are counted in bins of 1.0 density units.

Figure 5 presents the effect of distance-dependency on the fractions of different types of galaxies. The figure shows the fractions in the magnitude-limited sample as in Fig. 4, but separately for distances from 200 to $250 h^{-1}\text{Mpc}$, and from 290 to $340 h^{-1}\text{Mpc}$. The results are qualitatively similar: the fraction of star-forming galaxies drop and the fraction of passive galaxies rises when moving towards higher densities. This implies that although the exact values of the fractions of different types of galaxies depend on the sample volume, the phenomenon of observed environmental dependency is not caused by distance-related selection effects. In the higher distance interval, 290 to $340 h^{-1}\text{Mpc}$, there are fewer rich superclusters (Einasto et al. 2012a), and so the number of galaxies in the highest densities is small and random fluctuations become larger.

3.2. Group properties and environment

To study the group-scale effects on galaxies, we use richness N_{rich} and total luminosity L_r of the group as measures. They are correlated, but we can see in Fig. 6 that their relation depends on the large-scale density. The figure shows the average luminosity of groups as a function of group richness in four

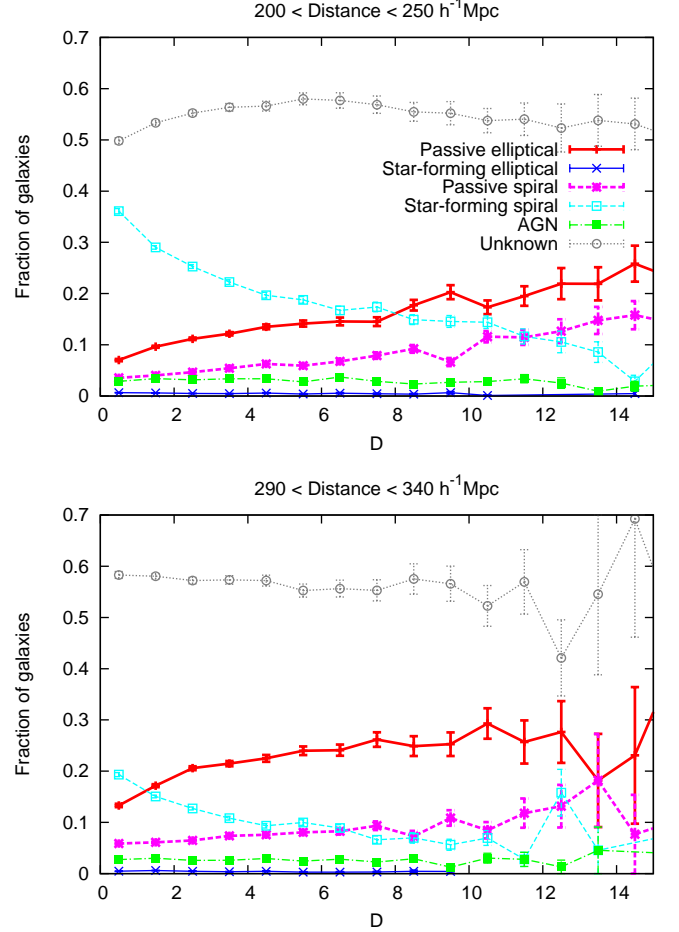


Fig. 5. Fractions of different samples of galaxies as a function of the large-scale environmental density, as in Fig. 4, but for magnitude-limited sample in two distance bins: 200 to $250 h^{-1}\text{Mpc}$ (top) and 290 to $340 h^{-1}\text{Mpc}$ (bottom).

large-scale density bins. Luminosities were calculated in richness bins of five galaxies. Groups in higher large-scale densities are on average more luminous when their richness is the same. This seems to imply that halo mass, which is strongly correlated with richness, does not completely explain the total luminosities of groups. The mass-to-luminosity ratio may depend on the large-scale environment. The main reason for this result is that the most luminous galaxies are more often in high-density environments. We showed in Fig. 3 that passive galaxies are on average in higher density large-scale environments than star-forming spirals. Since the most luminous galaxies are passive ellipticals, it is expected that average luminosities are higher in high-density regions.

Figure 7 shows the fractions of different samples of galaxies as a function of the group richness. The fractions are calculated in richness bins of five galaxies. The left-hand plot shows the results for galaxies in large-scale environments with density $D < 5.0$, while the right-hand plots show the results for galaxies in supercluster regions with density $D > 5.0$.

The fractions of different types of galaxies depend on their group-scale environment in the same way as their large-scale environment: the richer the group, the more passive galaxies it contains. The rise in the fraction of passive (red) galaxies as a function of richness in small groups has also been found by Hansen et al. (2009) and Weinmann et al. (2006). However,

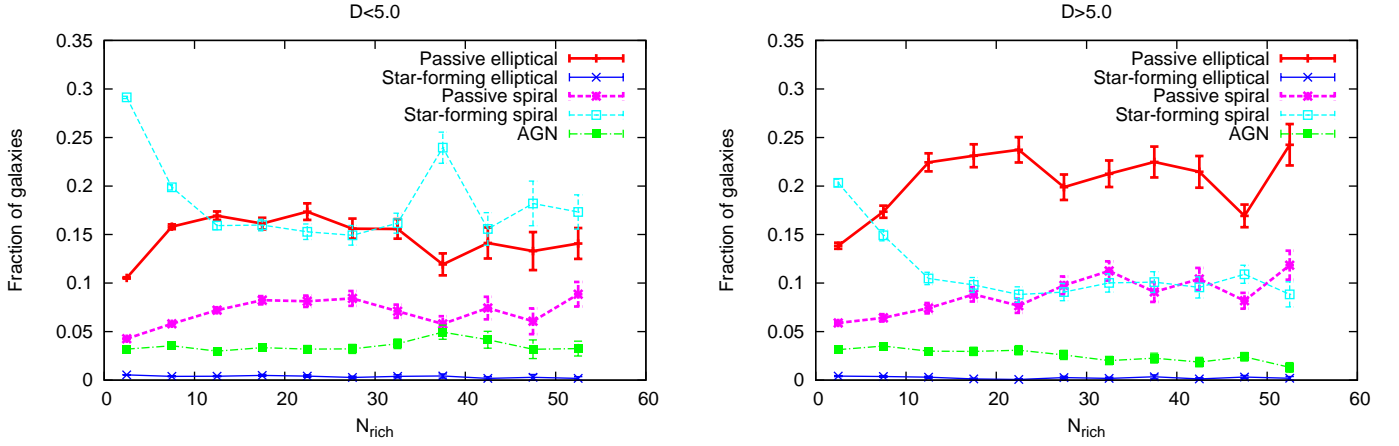


Fig. 7. Fractions of different samples of galaxies as a function of group richness in regions with lower density large-scale environment (left) and in superclusters (right). Error bars show the Poisson errors.

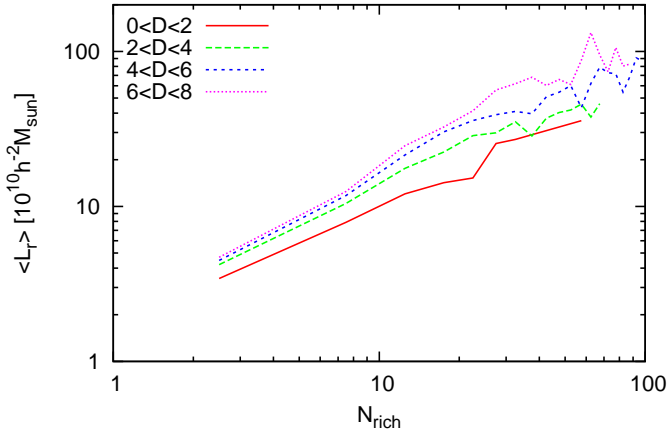


Fig. 6. Average luminosity for groups as a function of group richness in four large-scale density bins.

there is a difference between the supercluster environments and the low-density environments that can be seen even when the local environment is the same. In low-density environments the numbers of passive elliptical and star-forming spiral galaxies are equal in groups with ten or more galaxies, while in the supercluster environments the fraction of elliptical galaxies becomes larger. This result is in accordance with the results by Tempel et al. (2011) and Einasto et al. (2007). The fraction of passive spiral galaxies rises moderately with the group richness, but it does not depend on the large-scale environment. The fraction of AGN slightly decreases in supercluster environment, while in void or filament environment it is constant. This was also seen in Fig. 3.

The most prominent dependency on the environment is the difference between star-forming and passive galaxies. To study this in more detail, we calculated the fractions of all star-forming and passive galaxies regardless of their morphology. We divided these galaxies in four bins based on their large-scale environment: $0.0 < D < 2.0$ (typically voids), $2.0 < D < 4.0$ (filaments), $4.0 < D < 6.0$ (edges of superclusters), and $6.0 < D < 8.0$ (supercluster cores). The fractions of star-forming and passive galaxies as functions of group richness and group lu-

minosity in these density bins are shown in Fig. 8. To smooth the curves and improve the reliability, we used a binning of two galaxies in group richness. In all the bins of all samples up to group richness of ten galaxies the number of galaxies is more than a hundred. For luminosities, the fractions were calculated in bins of $5 \times 10^{10} h^{-2} L_{\odot}$.

The crossing point at which passive galaxies become more numerous than star-forming moves to lower group richness when the large-scale density grows. In low-density regions in groups of more than eight galaxies the fractions of passive and star-forming galaxies are approximately equal, while in higher density regions the fraction of passive galaxies gets higher, while the fraction of star-forming galaxies gets lower. When the large-scale density gets close to the supercluster limit ($D \sim 5$), increasing the density does not change the fractions any further. The dependence of the crossing point on the large-scale density can also be seen in luminosity, although the differences between the density levels are smaller.

The differences between the supercluster environment and the low-density environment may be due to different evolution between galaxies in high and low-density environments. Properties of galaxies that are characteristic to galaxies in early phases of their evolution are more often found in low-density environments. In Figs. 7 and 8 we can see that the group scale affects galaxies in the smallest groups. In richer groups the fractions of different types of galaxies are almost independent of group richness. A possible explanation for this is that in the small groups, the evolution is still in progress. Larger groups have been formed through mergers of smaller groups, and they are older and more mature structures.

We also calculated average $g - r$ colors of galaxies in different large-scale environments as a function of group richness. The results are shown in Fig. 9 for all galaxies, divided in the four bins of large-scale density. On average, galaxies are approximately 0.05 magnitudes redder in supercluster areas than in voids. The transition from star-forming to passive galaxies can be seen in galaxy colors. The average color gets redder when the group richness rises to ~ 10 galaxies. For richer groups, the color is independent on group richness, indicating that formation of these groups is more or less finished. However, this does not mean they are virialised, they can still contain substructures (Einasto et al. 2012b). The color-dependency found in Fig. 9 is caused by changes in the relative fractions of star-forming and

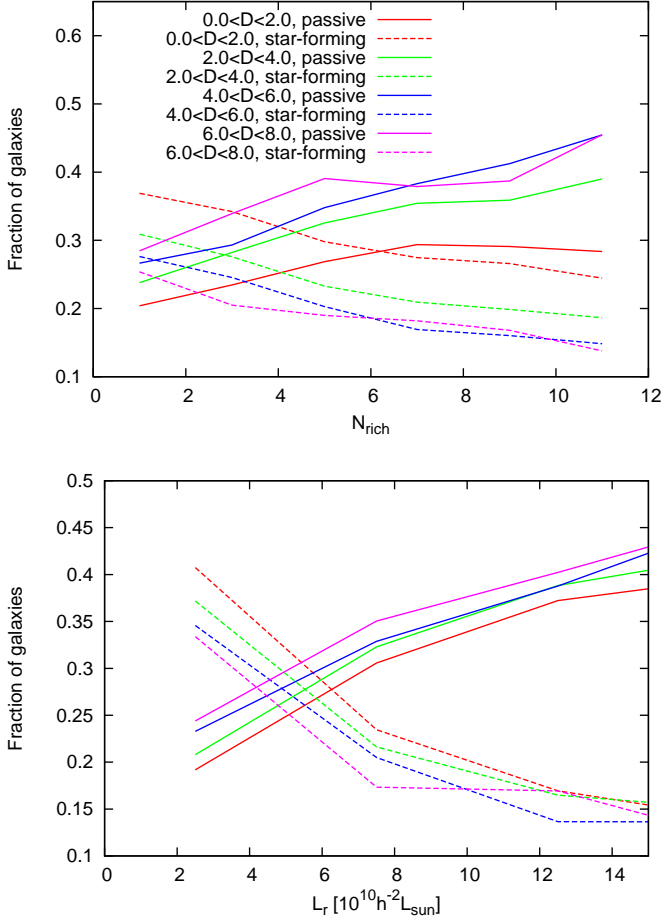


Fig. 8. Fractions of passive (solid lines) and star-forming (dashed line) galaxies as functions of group richness (top) and luminosity (bottom) in four large-scale density bins. The fractions are calculated in richness bins of two galaxies and luminosity bins of $5 \times 10^{10} h^{-2} L_{\odot}$.

passive galaxies. The colors of different types of galaxies do not depend on their environment on group or supercluster scale. The average colors are those presented in Table 1 regardless of environment. Therefore, the dependency between color and environment is another way to express the dependency between star-forming activity and the environment. Our results are consistent with other studies based on colors of galaxies (Hansen et al. 2009; Skibba 2009).

3.3. Distribution of galaxies in groups

To study the possible differences in radial distribution of elliptical and spiral galaxies in groups, we have analysed their three-dimensional spatial distribution around the center of the group. We have used the given group distance and the projected coordinates to calculate the group center (x_c, y_c, z_c), after which we measured the separation from this point for all the galaxies in the group. For galaxy distances we have used the co-moving distances where the finger-of-god effect is suppressed. To study all groups together and to evaluate the possible differences between galaxy types, we calculated the mean value of the separations for all galaxies in the groups. First we selected the data by the surrounding large-scale density $D < 5.0$, and divide the sample in two categories by distance: groups that are closer than

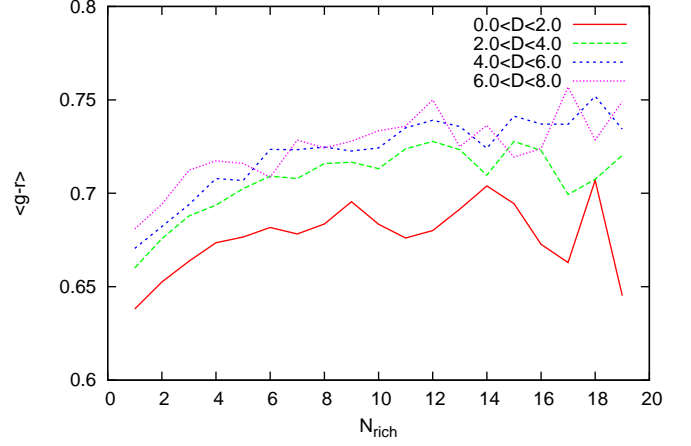


Fig. 9. Average $g-r$ color of galaxies as a function of richness of their group for galaxies in four bins of large-scale density.

$200 h^{-1} \text{Mpc}$ and groups that are beyond this region. Our analysis shows that there is no difference between the mean distances of galaxies in the groups as a function of distance. This is a good sign as this shows that there is no bias in the galaxy type distribution that would depend on the distance. All values we refer in the text later on, are for the whole sample. If we further divide the group sample to passive and star-forming galaxies and add another environment $D \geq 5.0$, we have four different galaxy populations in two different large-scale environments. The results show that elliptical galaxies and spiral galaxies are distributed in a different way. In the low density sample passive elliptical galaxies have a mean separation of $0.307 \pm 0.001 h^{-1} \text{Mpc}$, while the passive spiral galaxies are further away with the mean distance of $0.344 \pm 0.003 h^{-1} \text{Mpc}$. In the high density region the mean separations are larger: $0.617 \pm 0.006 h^{-1} \text{Mpc}$ for elliptical galaxies and $0.705 \pm 0.01 h^{-1} \text{Mpc}$ for spiral galaxies. The same feature is also observed among star forming galaxies and the referred values are approximately the same.

To further study if the mean separations depend on the number of members we made another test. The same surrounding densities were used, and groups of galaxies were divided to poor sample with $N_{\text{rich}} = 3$ or 5 and rich sample with $N_{\text{rich}} \geq 10$. The results was that in general both elliptical galaxies and spiral galaxies have larger mean distances in rich groups. For $N_{\text{rich}} = 3$ the mean distance is $\sim 0.2 h^{-1} \text{Mpc}$ and for $N_{\text{rich}} = 5$ the distance is $\sim 0.3 h^{-1} \text{Mpc}$ and for $N_{\text{rich}} \geq 10$ the distance is already $\sim 0.5 - 1.0 h^{-1} \text{Mpc}$. This was expected since richer groups are typically larger by size. Also in these samples the mean distances are larger for spiral galaxies than for elliptical galaxies. However, if we fix the number of members in the group, the separations do not depend as much on the large-scale density as before. Only in the $N_{\text{rich}} \geq 10$ sample there are notable differences in the mean distances for galaxies at different densities. Since the group richness has different distribution in different large-scale galaxy densities, the global mean values differ for large groups. These are interesting results showing importance of group richness to the mean distances of elliptical and spiral galaxies. Passive and starforming galaxies behave practically in the same way in most samples. Again, only for rich groups there are systematic differences in the mean distances. Star-forming galaxies have $\sim 16\%$ larger distances than those for passive galaxies.

4. Discussion

Our results support the conclusion of Bamford et al. (2009) and van der Wel et al. (2010), that color and structural parameters of galaxies depend differently on the environment. Star-forming galaxies have lower group richness and large-scale density than passive galaxies regardless of morphology. For spiral galaxies, the dependency of star-formation rate and the environment was also observed by Koopmann & Kenney (2004). Based on these studies we can conclude that what we observe as the morphology-density relation is mostly due to spiral galaxies being usually star-forming and elliptical galaxies passive.

Several mechanisms have been suggested for quenching star formation in galaxies. These include interactions between the galaxy and the surrounding intracluster medium (see review by van Gorkom 2004) and mergers of galaxies (Hopkins et al. 2008). Mergers are expected to happen in small groups. Sol Alonso et al. (2006) found that galaxy interactions are effective at triggering star-formation activity in low- and moderate-density environments. Different distribution of star-forming and passive galaxies in low and high-density environments hints that some environmental effect affects the quenching of star-formation. We found that passive galaxies with both, elliptical and spiral morphology prefer richer groups and higher large-scale densities than star-forming spirals. This result indicates that the environmental effects can quench star formation both, by changing the morphology of the galaxy from spiral to elliptical, and without affecting the morphology. Kauffmann et al. (2004) concluded that since the morphology does not depend on the environment, the trend in star formation cannot be driven by processes that alter structure, such as mergers or harassment.

According to our results, the fraction of AGN of all galaxies does not depend strongly on group richness or the large-scale environment. In Lietzen et al. (2011) radio quiet quasars and Seyfert galaxies, which were selected by the same criteria that we use here, were distributed predominantly in low-density environments. Based on the results in this paper, the radio-quiet AGN may reflect the overall distribution of galaxies. Lietzen et al. (2009) found that quasars have less neighboring galaxies than luminous inactive galaxies. The difference between their result and the one in this paper is due to their control sample, which consisted of very luminous galaxies. The most luminous galaxies are more likely to be located in high-density environments. On the other hand, our results agree with those of Silverman et al. (2009), who found that the fraction of group galaxies hosting an AGN is similar to field galaxies, and Martini et al. (2007) who found that AGN do not show any evidence of different substructure distribution than inactive galaxies in a cluster. The flat distribution of AGN (in Figs. 4 and 7) suggests that the environment does not have a strong effect on triggering AGN. We found small differences in the average large-scale density as a function of group richness of AGN compared to other types of galaxies (Fig. 3). This result may indicate that in regions with high large-scale density, AGN would be more likely in smaller groups than in regions with low large-scale density.

There are several studies which indicate that galaxy properties also depend on the large-scale environment in which they reside (e.g. Park et al. 2008; Cooper et al. 2010). In these studies the large-scale environment is often interpreted as relatively small regions around the object under study, kpc to a few Mpc. Here the large-scale environment refers to different density levels of the large-scale galaxy density field and its characteristics; superclusters and voids ranging scales from ten to a hundred Mpc. We found that the fractions of different types of galax-

ies depend on both, group richness and the large-scale density. *Galaxies in equally rich groups are more likely to be passive if they are in supercluster environments than if they are in low density region (Figs. 7 and 8).* This result implies that the large-scale environment affects the galaxy and group properties. A similar result was found by Einasto et al. (2008) for individual rich superclusters. They reported that in equally rich groups there are more early-type galaxies in supercluster cores than in the outskirts of superclusters. Also the galaxies that do not belong to any group are more often early-type if they are in supercluster cores.

Using spectroscopically identified compact group galaxies Scudder et al. (2012) showed that star-formation rates of star-forming galaxies are significantly different between isolated groups and groups embedded within a larger systems. Isolated groups with same stellar mass exhibit enhanced star formation relative to the embedded groups. Based on a statistical study of galaxies in voids and void walls in the SDSS and 2dFGRS catalogs, Ceccarelli et al. (2008) report that the galaxy population is also affected by large-scale modulation of star formation in galaxies. Sorrentino et al. (2006) studied galaxy properties in different large-scale environments in the SDSS DR4. They concluded that the fraction of late-type galaxies decreases and the fraction of early-type galaxies increases from underdense to denser environments. This transition is a smooth continuity of galaxy properties from voids to clusters. This implies that the method through which the environment affects the galaxies changes gradually with the increasing density rather than a phenomenon tied to a certain threshold density.

Einasto et al. (2005a) showed by numerical simulations that in void regions only poor systems are formed, and these systems grow very slowly. Most of the particles are maintained in their primordial form, remaining non-clustered. In superclusters the dynamical evolution is rapid and starts earlier, consisting a continua of transitions of dark matter particles to building blocks of galaxies, groups, and clusters. Moreover, dark matter halos in voids are found to be less massive, less luminous, and their growth of mass is suppressed and stops at earlier epoch than in high-density regions. The merger rate is a function of the environmental density (Gottlöber et al. 2003; Colberg et al. 2005; Einasto et al. 2005a; Fakhouri & Ma 2009). Tempel et al. (2009) showed that during the structure formation of the Universe, halo sizes in the supercluster core regions increase by many factors, while in void regions, halo sizes remain unchanged. Thus during the evolution of structure the overall density in voids decreases, and that suppresses the evolution of the small-scale protohalos in voids and low density regions.

Kereš et al. (2005) used hydrodynamical simulations to study hot and cold gas supply to the galaxies. They concluded that cold and hot gas modes depend on galaxy redshift and environment. Cold gas which dominated at high redshifts and low density regions nowadays may have important contribution for the star-formation rate in low mass systems. Cowie et al. (1996) found evidence of a cosmic downsizing: during the structure formation galaxies transform from star-forming stage to passive. Cen (2011) showed through hydrodynamical simulations that for galaxies at $z=0$ star formation is efficient in low density regions while it is substantially suppressed in the cluster environments. During the hierarchical structure formation, gas is heated in high density regions (groups, clusters, and superclusters) and every time larger fraction of the gas end up too hot (high entropy) phase to continue feeding the residing galaxies. As a result cold gas supply to galaxies in these regions is suppressed. The net effect is that star formation gradually shifts from larger halos

which populate overdense regions to the lower density environments. Thus lack of cold gas due to gravitational heating in dense regions may provide physical explanation for cosmic downsizing and one of its manifestations observed as color-density relation.

This evolution predicted by numerical simulations might be seen in the observational results of this paper. Our results imply that the environment may affect the galaxy evolution and properties on two overlapping levels. At the first level, via large-scale density field, which affects the evolution of galaxy and group size halos depending on field density. At the second, more local level, via gas supply together with baryonic and gravitational processes in groups that host galaxies. Figure 8 can also be interpreted as an evidence that galaxies in lower-density regions developed later than galaxies in similar mass groups in high-density environments. This can be studied in more detail through the assembly history of groups in numerical simulations.

5. Summary and conclusions

In this paper, we have studied the environments of galaxies of the SDSS DR8 between distances 120 and $340 h^{-1}$ Mpc. We divided the galaxies in different samples based on their spectral properties and morphology. We measured the large-scale environment using a luminosity-density field, and the group-scale environment with the group richness. Our main results are the following:

- Passive galaxies are located in denser large-scale environments than star-forming galaxies. There is no significant difference between passive elliptical and passive spiral galaxies.
- The fraction of galaxies that are star-forming declines, and the fraction of passive galaxies rises when the richness of a group rises from one to approximately ten galaxies. In groups with richness between 20 and 50 galaxies, the fractions of different types of galaxies do not depend on group richness.
- The group richness at which the passive galaxies become more numerous than the star-forming depends on the large-scale environment. When the large-scale density grows from levels typical to voids to supercluster regions the group richness where most galaxies become passive declines. Also the level of fractions of star-forming and passive galaxies in rich groups depends on the large-scale environment: in voids the numbers of passive and star-forming galaxies stay approximately equal in groups with more than 10 galaxies, while in superclusters the fraction of passive galaxies is considerably larger.
- Equally rich groups are more luminous in supercluster regions than in voids.
- The fraction of galaxies with an AGN does not depend strongly on group richness or the large-scale density.

We conclude that the galaxy evolution is affected both, by the group where the galaxy resides, and by its large-scale environment. As a next step we are planning to use numerical simulations to study the plausible baryonic and gravitational processes that determine the galaxy evolution in groups of galaxies in different large-scale environments. Our another important approach is to study more detail groups observables which are known to characterise groups physical properties e.g. H I content, stellar mass, and X-ray properties.

Acknowledgements. We thank the referee, Ramin Skibba, for his useful comments that greatly helped to improve this paper.

H. Lietzen was supported by the Finnish Cultural Foundation and Emil Aaltonen's foundation.

The present study was supported by the Estonian Science Foundation grants No. 8005, 7765, 9428, and MJD272, by the Estonian Ministry for Education and Science research project SF0060067s08, and by the European Structural Funds grant for the Centre of Excellence "Dark Matter in (Astro)particle Physics and Cosmology" TK120.

Funding for the SDSS and SDSS-II has been provided by the Alfred P. Sloan Foundation, the Participating Institutions, the National Science Foundation, the U.S. Department of Energy, the National Aeronautics and Space Administration, the Japanese Monbukagakusho, the Max Planck Society, and the Higher Education Funding Council for England. The SDSS Web Site is <http://www.sdss.org/>.

The SDSS is managed by the Astrophysical Research Consortium for the Participating Institutions. The Participating Institutions are the American Museum of Natural History, Astrophysical Institute Potsdam, University of Basel, University of Cambridge, Case Western Reserve University, University of Chicago, Drexel University, Fermilab, the Institute for Advanced Study, the Japan Participation Group, Johns Hopkins University, the Joint Institute for Nuclear Astrophysics, the Kavli Institute for Particle Astrophysics and Cosmology, the Korean Scientist Group, the Chinese Academy of Sciences (LAMOST), Los Alamos National Laboratory, the Max-Planck-Institute for Astronomy (MPIA), the Max-Planck-Institute for Astrophysics (MPA), New Mexico State University, Ohio State University, University of Pittsburgh, University of Portsmouth, Princeton University, the United States Naval Observatory, and the University of Washington.

References

- Aihara, H., Allende Prieto, C., An, D., et al. 2011, *ApJS*, 193, 29
- Baldry, I. K., Balogh, M. L., Bower, R. G., et al. 2006, *MNRAS*, 373, 469
- Balogh, M. L., Baldry, I. K., Nichol, R., et al. 2004, *ApJ*, 615, L101
- Bamford, S. P., Nichol, R. C., Baldry, I. K., et al. 2009, *MNRAS*, 393, 1324
- Berlind, A. A., Frieman, J., Weinberg, D. H., et al. 2006, *ApJS*, 167, 1
- Blanton, M. R. & Berlind, A. A. 2007, *ApJ*, 664, 791
- Blanton, M. R., Eisenstein, D., Hogg, D. W., Schlegel, D. J., & Brinkmann, J. 2005, *ApJ*, 629, 143
- Blanton, M. R., Hogg, D. W., Bahcall, N. A., et al. 2003, *ApJ*, 592, 819
- Blanton, M. R. & Roweis, S. 2007, *AJ*, 133, 734
- Brinchmann, J., Charlot, S., White, S. D. M., et al. 2004, *MNRAS*, 351, 1151
- Ceccarelli, L., Padilla, N., & Lambas, D. G. 2008, *MNRAS*, 390, L9
- Cen, R. 2011, *ApJ*, 741, 99
- Colberg, J. M., Sheth, R. K., Diaferio, A., Gao, L., & Yoshida, N. 2005, *MNRAS*, 360, 216
- Cooper, M. C., Gallazzi, A., Newman, J. A., & Yan, R. 2010, *MNRAS*, 402, 1942
- Cowie, L. L., Songaila, A., Hu, E. M., & Cohen, J. G. 1996, *AJ*, 112, 839
- Dressler, A. 1980, *ApJ*, 236, 351
- Einasto, J., Hütsi, G., Einasto, M., et al. 2003, *A&A*, 405, 425
- Einasto, J., Tago, E., Einasto, M., et al. 2005a, *A&A*, 439, 45
- Einasto, M. & Einasto, J. 1987, *MNRAS*, 226, 543
- Einasto, M., Einasto, J., Tago, E., et al. 2007, *A&A*, 464, 815
- Einasto, M., Liivamägi, L. J., Tempel, E., et al. 2012a, *ArXiv e-prints* 1204.0933
- Einasto, M., Saar, E., Martínez, V. J., et al. 2008, *ApJ*, 685, 83
- Einasto, M., Suhhonenko, I., Heinämäki, P., Einasto, J., & Saar, E. 2005b, *A&A*, 436, 17
- Einasto, M., Vennik, J., Nurmi, P., et al. 2012b, *A&A*, 540, A123
- Fakhouri, O. & Ma, C.-P. 2009, *MNRAS*, 394, 1825
- Fukugita, M., Nakamura, O., Turner, E. L., Helmboldt, J., & Nichol, R. C. 2004, *ApJ*, 601, L127
- Gómez, P. L., Nichol, R. C., Miller, C. J., et al. 2003, *ApJ*, 584, 210
- Gottlöber, S., Łokas, E. L., Klypin, A., & Hoffman, Y. 2003, *MNRAS*, 344, 715
- Gunn, J. E. & Gott, III, J. R. 1972, *ApJ*, 176, 1
- Haas, M. R., Schaye, J., & Jeon-Daniel, A. 2011, *MNRAS*, 1812
- Hamilton, A. J. S. 1988, *ApJ*, 331, L59
- Hansen, S. M., Sheldon, E. S., Wechsler, R. H., & Koester, B. P. 2009, *ApJ*, 699, 1333
- Hickox, R. C., Jones, C., Forman, W. R., et al. 2009, *ApJ*, 696, 891
- Hopkins, P. F., Hernquist, L., Cox, T. J., & Kereš, D. 2008, *ApJS*, 175, 356
- Huertas-Company, M., Aguerri, J. A. L., Bernardi, M., Mei, S., & Sánchez Almeida, J. 2011, *A&A*, 525, A157
- Kauffmann, G., Heckman, T. M., Tremonti, C., et al. 2003, *MNRAS*, 346, 1055
- Kauffmann, G., White, S. D. M., Heckman, T. M., et al. 2004, *MNRAS*, 353, 713
- Kereš, D., Katz, N., Weinberg, D. H., & Davé, R. 2005, *MNRAS*, 363, 2
- Kewley, L. J., Dopita, M. A., Sutherland, R. S., Heisler, C. A., & Trevena, J. 2001, *ApJ*, 556, 121

- Komatsu, E., Smith, K. M., Dunkley, J., et al. 2011, *ApJS*, 192, 18
- Koopmann, R. A. & Kenney, J. D. P. 2004, *ApJ*, 613, 851
- Larson, R. B., Tinsley, B. M., & Caldwell, C. N. 1980, *ApJ*, 237, 692
- Lietzen, H., Heinämäki, P., Nurmi, P., et al. 2011, *A&A*, 535, A21
- Lietzen, H., Heinämäki, P., Nurmi, P., et al. 2009, *A&A*, 501, 145
- Liivamägi, L. J., Tempel, E., & Saar, E. 2012, *A&A*, 539, A80
- Martini, P., Mulchaey, J. S., & Kelson, D. D. 2007, *ApJ*, 664, 761
- Moore, B., Katz, N., Lake, G., Dressler, A., & Oemler, A. 1996, *Nature*, 379, 613
- Muldrew, S. I., Croton, D. J., Skibba, R. A., et al. 2012, *MNRAS*, 419, 2670
- Park, C., Gott, III, J. R., & Choi, Y.-Y. 2008, *ApJ*, 674, 784
- Pasquali, A., van den Bosch, F. C., Mo, H. J., Yang, X., & Somerville, R. 2009, *MNRAS*, 394, 38
- Porter, S. C., Raychaudhury, S., Pimbblet, K. A., & Drinkwater, M. J. 2008, *MNRAS*, 388, 1152
- Postman, M. & Geller, M. J. 1984, *ApJ*, 281, 95
- Press, W. H. & Davis, M. 1982, *ApJ*, 259, 449
- Scudder, J. M., Ellison, S. L., & Mendel, J. T. 2012, *MNRAS*, 423, 2690
- Silverman, J. D., Kovač, K., Knobel, C., et al. 2009, *ApJ*, 695, 171
- Skibba, R. A. 2009, *MNRAS*, 392, 1467
- Skibba, R. A., Bamford, S. P., Nichol, R. C., et al. 2009, *MNRAS*, 399, 966
- Sol Alonso, M., Lambas, D. G., Tissera, P., & Coldwell, G. 2006, *MNRAS*, 367, 1029
- Sorrentino, G., Antonuccio-Delogu, V., & Rifatto, A. 2006, *A&A*, 460, 673
- Tago, E., Einasto, J., Saar, E., et al. 2008, *A&A*, 479, 927
- Tago, E., Saar, E., Tempel, E., et al. 2010, *A&A*, 514, A102
- Tempel, E., Einasto, J., Einasto, M., Saar, E., & Tago, E. 2009, *A&A*, 495, 37
- Tempel, E., Saar, E., Liivamägi, L. J., et al. 2011, *A&A*, 529, A53
- Tempel, E., Tago, E., & Liivamägi, L. J. 2012, *A&A*, 540, A106
- Turner, E. L. & Gott, III, J. R. 1976, *ApJS*, 32, 409
- van der Wel, A., Bell, E. F., Holden, B. P., Skibba, R. A., & Rix, H.-W. 2010, *ApJ*, 714, 1779
- van Gorkom, J. H. 2004, *Clusters of Galaxies: Probes of Cosmological Structure and Galaxy Evolution*, 305
- Weinmann, S. M., van den Bosch, F. C., Yang, X., & Mo, H. J. 2006, *MNRAS*, 366, 2
- Wilman, D. J., Zibetti, S., & Budavári, T. 2010, *MNRAS*, 406, 1701
- Wolf, C., Aragón-Salamanca, A., Balogh, M., et al. 2009, *MNRAS*, 393, 1302
- Yang, X., Mo, H. J., van den Bosch, F. C., et al. 2007, *ApJ*, 671, 153
- York, D. G., Adelman, J., Anderson, Jr., J. E., et al. 2000, *AJ*, 120, 1579
- Zandivarez, A. & Martínez, H. J. 2011, *MNRAS*, 415, 2553